

Tower-foot Grounding Model for EMT programs Based on Transmission Line Theory and Marti's Model

Rafael Alipio, Alberto De Conti, Felipe Vasconcellos, Fernando Moreira, Naiara Duarte, José Martí

Abstract-- This paper proposes a tower-foot grounding system model compatible with EMT programs which might be useful for the simulation of lightning transients in overhead lines. The proposed model is based on the solution of the telegrapher's equations and the application of the classical Marti's transmission line model. The model is implemented in the Alternative Transients Program (ATP) and validated considering a benchmark electromagnetic model. Its accuracy is evaluated and shown both in terms of the simulated ground potential rise (GPR) and line overvoltages developed through the insulator strings due to lightning currents. Finally, the model accuracy is also demonstrated in terms of the line backflashover outage rate.

Keywords: Lightning transients, transmission lines, EMT programs, grounding, transmission line theory.

I. INTRODUCTION

FOR most overhead power transmission lines (TLs), lightning is the primary cause of unscheduled interruptions [1]. The assessment of the lightning performance of overhead TLs involves the calculation of the minimum lightning currents causing insulation flashover for strikes to phase conductors (shielding failure flashover) and to towers and shield wires (backflashover) [2]. Although the tower-foot

grounding system does not affect the occurrence of shielding failure flashover, it does affect the backflashover by markedly changing the amplitude and steepness of the resulting overvoltages across line insulators [3].

Typically, the assessment of the lightning performance of transmission lines is carried out using time-domain transient simulators [4], [5]. Such platforms, however, do not have specific models for the tower-foot grounding system. Thus, in most cases, the grounding system is normally modeled simply as a lumped resistance. This approach disregards the frequency-dependent behavior of grounding input impedance which might be important in lightning transients [6]. An alternative and more accurate approach is the determination of the frequency-dependent response of the tower-foot grounding externally using an electromagnetic field approach and then including it in the time-domain simulator through a pole-residue representation [7], [8]. This second approach, however, is more laborious and time consuming. A third approach, which balances accuracy and computational effort, is the representation of the grounding electrodes as a buried transmission line. This approach, however, is generally used only for representing simple arrangements such as single horizontal or vertical grounding electrodes [9], [10]. In [11], a pi-equivalent circuit model was proposed to represent general grounding system arrangements of transmission lines, based on an accurate circuit model and an optimization procedure to determine the pi-circuit parameters. Recently, the tower-foot grounding modeling through a lumped resistance with the same value as the so-called grounding impulse impedance was also suggested [3].

In this paper, a tower-foot grounding model based on the solution of the telegrapher's equations is proposed and implemented in the Alternative Transients Program (ATP) using the classical Marti's transmission line model [12]. The accuracy of the proposed model is evaluated using an electromagnetic model as a benchmark. The obtained results serve as a basis for implementing an electrical grounding component in time-domain simulators which might benefit the industry, allowing more accurate simulations of lightning overvoltages in overhead TLs. Thus, the main novelty of this paper consists in the use of a stable model widely available in EMT-type platforms, namely the FDLIne model or Marti's model, to simulate the transient response of grounding electrodes together with other electrical system components.

This paper is organized as follows. In Section II the case study consisting of a 138-kV line is presented. The proposed model for the tower-foot grounding system, along with its

This work was supported in part by Conselho Nacional de Desenvolvimento Científico e Tecnológico (CNPq) under Grants 306006/2019-7, 314849/2021-1 and 406177/2021-0, in part by Fundação de Amparo à Pesquisa do Estado de Minas Gerais (FAPEMIG) under Grants TEC-PPM-00280-17 and APQ-01081-21, in part by Federal Commission for Scholarships for Foreign Students for the Swiss Government Excellence Scholarship (ESKAS No. 2022.0099), and in part by Swiss National Science Foundation (SNSF) under Grant TMPFP2_209700.

R. Alipio is with the Electromagnetic Compatibility Laboratory, Swiss Federal Institute of Technology in Lausanne (EPFL), 1015, Switzerland, on leave from the Federal Center of Technological Education of Minas Gerais (email: rafael.alipio@cefetmg.br).

A. De Conti is with the Department of Electrical Engineering, Federal University of Minas Gerais, Belo Horizonte, MG, Brazil (e-mail: conti@cpdee.ufmg.br).

F. Vasconcellos is with the Department of Electrical and Computer Engineering, Federal University of Bahia, Salvador, BA, Brazil (email: felipe.vasconcellos@ufba.br).

F. Moreira is with the Department of Electrical and Computer Engineering, Federal University of Bahia, Salvador, BA, Brazil (email: moreiraf@ufba.br).

N. Duarte is with the Laboratory of Electromagnetic Transients, Federal Center of Technological Education, Belo Horizonte, MG, Brazil (e-mail: naiara.duarte@gmail.com).

J. R. Martí is with the Electrical and Computer Engineering Department, University of British Columbia, Vancouver, Canada (e-mail: jrms@ece.ubc.ca).

implementation in ATP and validation using a benchmark electromagnetic model, is presented in Section III. In Section IV the proposed tower-foot grounding model is applied to assess the lightning performance of the studied transmission line. Finally, Section V presents the main conclusions of the paper and makes a summary of it.

II. CASE STUDY

In the developments of this work, a case study corresponding to a typical 138-kV transmission line is considered. Fig. 1 shows the tower geometry, taken from [8], which has one ACSR conductor per phase (LINNET) and one 3/8" EHS shield wire.

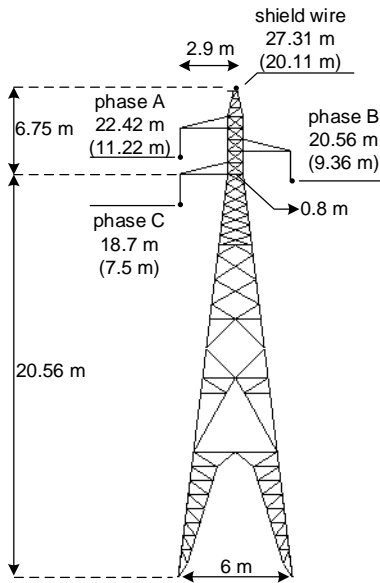


Fig. 1. Tower geometry of the tested 138-kV line [8].

In the analysis of the lightning performance of overhead TLs, the response to first return stroke currents associated with downward flashes is the most relevant aspect [5]. In the simulation results presented in this paper, the current waveform shown in Fig. 2 is assumed. This waveform is modeled as the sum of Heidler's functions, as detailed in [13], and closely reproduces the median parameters of downward negative first return strokes measured at Mount San Salvatore station [14], which is assumed as the international reference for lightning-related studies [15]. The first-stroke current is characterized by a peak value of 31 kA and a virtual front time (calculated as the time between 30% and 90% of its peak value, divided by 0.6) of 3.8 μ s.

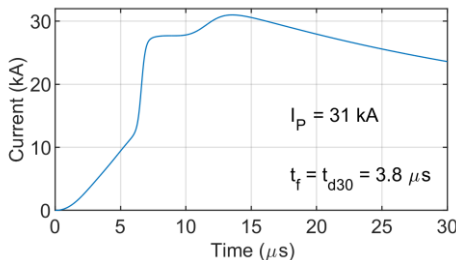


Fig. 2. Representative lightning current waveform of first strokes measured at Mount San Salvatore [13], [14].

III. TOWER-FOOT GROUNDING MODELING USING TRANSMISSION LINE THEORY AND MARTI'S MODEL

A. Per-unit-length Parameter Calculation

Fig. 3 shows the typical electrode arrangement of the transmission line tower grounding. It consists of four bare conductors, known as counterpoise wires, that are buried on a depth h and are laid parallel to the surface of the earth. The grounding electrodes start from the tower legs at a 45 degrees angle. After reaching a length ℓ_1 , they change their direction and become parallel to the right-of-way. The length ℓ_2 of the counterpoise wires running parallel to each other is adjusted to maximize the effectiveness of the grounding system according to the soil resistivity value. This means that the total length $\ell = \ell_1 + \ell_2$ of each counterpoise wire is set such that the effective length of the grounding system is not exceeded.

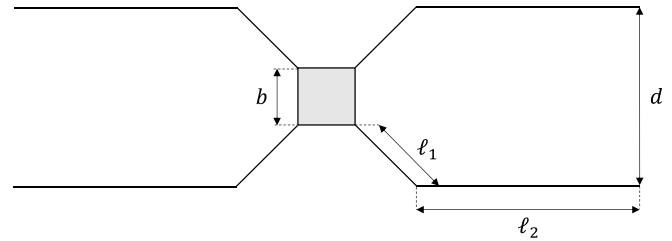


Fig. 3. Tower-foot grounding.

From a theoretical standpoint, the four counterpoise wires are electromagnetically coupled and therefore a rigorous electromagnetic model should be used for their representation. However, a transmission line model may be adopted as long as some assumptions are made. First, the symmetry of the problem is taken into consideration and only the wires at one side of the tower are considered electromagnetically coupled. Second, each pair of wires is modeled using an equivalent uniform transmission line representation characterized by the following equations

$$\frac{dV}{dx} = -Z_i - j\omega LI \quad (1)$$

$$\frac{dI}{dx} = -(G + j\omega C)V \quad (2)$$

where V and I are voltage and current vectors of size 2×1 , Z_i and L are 2×2 matrices respectively containing the internal impedance of the conductors and the external inductance per unit length, G and C are 2×2 matrices respectively containing the shunt conductance and capacitance per unit length and ω is the angular frequency.

Matrix G is the inverse of the shunt resistance matrix R , whose main-diagonal elements R_s are identical. These elements are calculated using the equation proposed by Sunde for determining the grounding resistance of a buried bare conductor parallel to the surface of the earth [16]

$$R_s = \frac{1}{\pi\sigma_g} \left[\ln \left(\frac{2\ell}{\sqrt{2hr}} \right) - 1 \right] \quad (3)$$

where σ_g is the ground conductivity, ℓ is the total counterpoise length, $h = 0.8$ m is the burial depth, and $r = 4.7625$ mm is the counterpoise radius.

The mutual shunt resistance R_M corresponding to the off-

diagonal elements of \mathbf{R} is proposed here to be calculated as

$$R_M = \frac{e^{-\gamma_g \bar{d}}}{\pi \sigma_g} \left[\ln \left(\frac{2\ell}{\sqrt{2h\bar{d}}} \right) - 1 \right] \quad (4)$$

where $\gamma_g = \sqrt{j\omega\mu_0(\sigma_g + j\omega\epsilon_g)}$ is the intrinsic propagation constant of the ground, in which ϵ_g is the ground permittivity and μ_0 is the vacuum permeability, and \bar{d} is given by

$$\bar{d} = \frac{d_1 \ell_1 + d_2 \ell_2}{\ell} \quad (5)$$

where $d_1 = (b + d)/2$ is the average horizontal separation between the diagonally oriented parts of the grounding electrodes, $d_2 = d = 20$ m is the total electrode separation, and $b = 6$ m is the tower base width. The exponential term is introduced in (4) to account for the propagation delay in the transversal direction. Once \mathbf{R} is determined with (3) and (4), the shunt conductance and shunt admittance matrices per unit length are simply calculated as $\mathbf{G} = \mathbf{R}^{-1}$ and $\mathbf{C} = (\epsilon_g/\sigma_g)\mathbf{G}$ [17].

It is worth mentioning that expression (4) for calculating the mutual shunt resistance, except for the exponential term, has been shown to be a good approximation for calculating the mutual effects between parallel electrodes with geometry as illustrated in Fig. 3, based on comparisons with several other models available in the literature [18], [19]. This expression is obtained from (3) by replacing the conductor radius by the distance between the electrodes and the depth by the average depth of the electrodes.

The internal impedance \mathbf{Z}_i in (1) is a diagonal matrix that can be usually neglected in grounding impedance calculations. However, it was included for completeness considering the exact solution for the internal impedance of a solid cylindrical conductor [20]. Finally, the diagonal elements L_S of matrix \mathbf{L} are calculated using [17], [21]

$$L_S = \frac{\mu_0}{2\pi} \left[\ln \left(\frac{2\ell}{\sqrt{2hr}} \right) - 1 \right] \quad (6)$$

while the off-diagonal elements L_M of \mathbf{L} , following an approach that is similar to the one adopted to compute the mutual shunt resistance, are proposed here to be calculated as

$$L_M = \frac{\mu_0}{2\pi} \left[\ln \left(\frac{2\ell_2}{\sqrt{2hd}} \right) - 1 \right] e^{-\gamma_g d} \quad (7)$$

It must be noted that only the length ℓ_2 related to the extension of the grounding electrodes that run parallel to each other is considered in (7). Moreover, the distance between the electrodes is that between the parallel section (d) and not the average horizontal separation (\bar{d}). This is so because the non-parallel sections of the counterpoise wires are orthogonal and therefore not magnetically coupled. As in (4), equation (7) includes an exponential term that accounts for the propagation delay in the transversal direction. Since equations (3)-(7) assume a homogeneous ground, the ground conductivity in (3) and (4) should be viewed as an apparent value intended to represent a multilayer ground equivalently. For representing a multilayer ground structure in detail, equations (3)-(7) should be modified accordingly.

As discussed in [22], the transmission line approximation should be valid for buried wires provided the ground-return currents are confined in a region delimited by the wavelength

in the ground. The following approximate expression is proposed in the same reference to determine the frequency limit, in Hz, below which the transmission line approximation should be valid

$$f_{max} = \frac{\mu_0 \sigma_g \pi c^2}{\sqrt{\epsilon_{rg} \{ \epsilon_{rg} + \mu_0 \epsilon_g [2\pi c]^2 \}}} \quad (8)$$

where ϵ_{rg} is the ground relative permittivity and c is the speed of light. Equation (8) predicts an inverse relationship between the ground resistivity $\rho_g = 1/\sigma_g$ and f_{max} . For example, for a constant ground resistivity of 250 Ωm and a ground relative permittivity of 10, this expression leads to $f_{max} = 22$ MHz, which greatly exceeds the range of frequencies expected to occur in lightning overvoltages. If the ground resistivity is increased to 5000 Ωm , this frequency limit is reduced to 1.1 MHz, which still covers the range of frequencies in which the bulk of the lightning energy is confined. If a more realistic frequency-dependent soil model is used, these limiting values will increase due to the reduction of the soil resistivity with frequency. This indicates that (1) and (2) can be used to model counterpoise wires with sufficient accuracy within the limits of transmission line theory.

B. ATP Modeling of the Grounding Electrodes

Since the matrices \mathbf{G} , \mathbf{C} , \mathbf{Z}_i , and \mathbf{L} are symmetric and perfectly balanced, a real and constant transformation matrix can be conveniently used to diagonalize the transmission line equations (1) and (2) and write them in the modal domain in exact form. By defining $\mathbf{I} = \mathbf{T}_I \mathbf{I}_m$ and $\mathbf{V} = \mathbf{T}_V \mathbf{V}_m$, where \mathbf{I}_m and \mathbf{V}_m are the modal-domain equivalents of \mathbf{I} and \mathbf{V} , respectively, and observing that $\mathbf{T}_V^t = \mathbf{T}_I^{-1}$ [23], the transformation matrix \mathbf{T}_I can be simply written as

$$\mathbf{T}_I = \frac{1}{\sqrt{2}} \begin{bmatrix} 1 & 1 \\ 1 & -1 \end{bmatrix} \quad (9)$$

After transformation to the modal domain, equations (1) and (2) can be accurately solved in the time domain using Marti's transmission line model [12] implemented in ATP. However, there is no model in ATP to calculate the per-unit-length parameters considering the equations presented in the previous section. For this reason, the line parameters were calculated in Matlab. The rational fitting of the characteristic impedance and propagation function of each mode required in Marti's model was also performed in Matlab. This was done using the vector fitting technique [24] considering real poles only. The poles and residues obtained from the fitting as well as the transformation matrix \mathbf{T}_i were written as a text file with the extension .pch and coupled with ATP following the approach described in detail in [25]. Using this approach, each pair of counterpoise wires shown in Fig. 3 can be modeled in ATP as a two-phase transmission line with Marti's model.

C. Model Validation

To demonstrate the validity of the transmission line modeling of the counterpoise wires using the approach

proposed in this paper, simulations were performed considering the realistic current waveform shown in Fig. 2. In the simulations, the sending ends of the four counterpoise wires shown in Fig. 3 were connected to a single virtual node representing the tower bottom. An ideal current source injected the lightning return-stroke current at this node and the resulting ground potential rise (GPR) was calculated. Five low-frequency values of ground resistivity were considered, namely 250, 500, 1000, 2500, and 5000 Ωm . In all cases, the ground resistivity and permittivity were assumed to vary with frequency according to the Alipio-Visacro model [26]. The total length of each counterpoise wire was changed so that the effective length corresponding to each ground resistivity was not exceeded. The considered values are listed in Table I.

TABLE I
LENGTH OF THE COUNTERPOISE WIRES AS A FUNCTION OF LOW-FREQUENCY GROUND RESISTIVITY

ρ_g (Ωm)	250	500	1000	2500	5000
ℓ (m)	15	25	40	55	80

Figs. 4 and 5 illustrate the absolute values of the modal characteristic impedance and the modal propagation function, respectively, associated with the counterpoise wires for ground resistivities of 250 Ωm and 2500 Ωm . Also shown in the figures are the fitted curves obtained with the vector fitting technique. These values were selected because they demonstrate the overall behavior of both parameters for the conditions indicated in Table I.

In general, a good agreement is observed in Fig. 4 and Fig. 5 between the original and fitted curves. However, the fitting of the model parameters with real poles as required in the ATP implementation of Marti's model becomes increasingly difficult with increasing values of ground resistivity and frequency. For this reason, although the fitting for the 250- Ωm and 500- Ωm soils could be performed up to 10 MHz, for ground resistivities equal to or greater than 1000 Ωm the fitting had to be limited to 1 MHz for best accuracy. Nevertheless, the performance of the grounding models was not severely affected because most of the energy associated with the return stroke current of Fig. 2 (and most lightning currents, in general) is well below 1 MHz.

Model passivity was checked by assuring that [27]

$$\text{eig}((Y_n + Y_n^H)/2) > 0 \quad \forall s, \quad s = j\omega \quad (10)$$

where Y_n is the nodal admittance matrix calculated from the fitted propagation function and characteristic admittance of the line, and superscript 'H' corresponds to the Hermitian of a matrix. In all cases indicated in Table I, the inequality in (10) was confirmed for frequencies up to 10 MHz even if the model was accurately fitted up to 1 MHz only. This was done to investigate the occurrence of out-of-band passivity violations. In none of the cases any passivity violation was identified.

Fig. 6 illustrates the GPRs calculated with the implemented grounding models. Also included in the figure are voltage waveforms calculated using the hybrid electromagnetic model

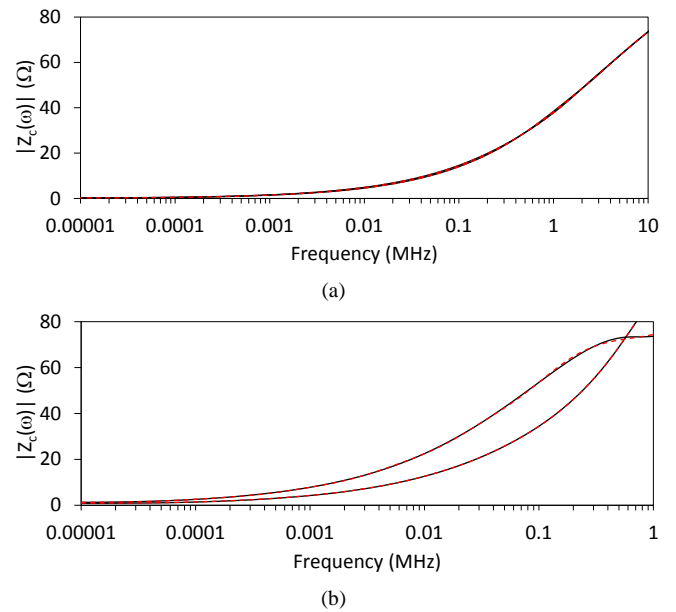


Fig. 4. Absolute value of the modal characteristic impedance $Z_c(\omega)$ of the counterpoise wire model for soil resistivities of (a) 250 Ωm and (b) 2500 Ωm . Black solid lines: original curves; red dashed lines: fitted curves.

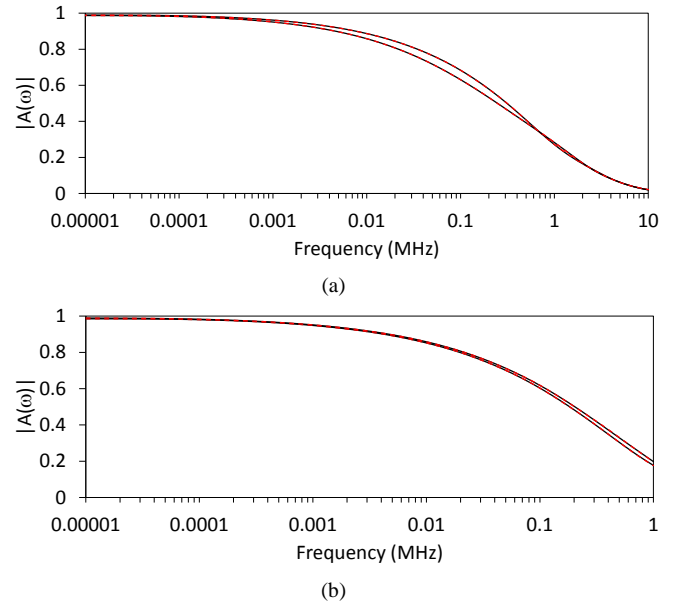


Fig. 5. Absolute value of the modal propagation function $A(\omega)$ of the counterpoise wire model for soil resistivities of (a) 250 Ωm and (b) 2500 Ωm . Black solid lines: original curves; red dashed lines: fitted curves.

(HEM) [28], which provides a rigorous solution to the problem by considering the electromagnetic coupling of a system of arbitrarily oriented electrodes in the solution of the scalar potential and magnetic vector potential equations derived from Maxwell's equations. As discussed in detail in [29], its acronym HEM reflects the hybrid electromagnetic-circuit approach of the model, since its formulation is based on EM theory to compute the coupling among grounding electrodes from a numerical implementation of basic EM equations (including propagation effects) and its results are expressed in terms of circuit quantities such as voltages and currents. It is noteworthy that the HEM model was extensively validated considering experimental results of the impulse

response of different grounding configurations [30], [31].

As seen in Fig. 6, the agreement between the waveforms calculated with the different methods is excellent in all cases. The most significant deviations are observed for the 250 Ωm ground resistivity. However, they do not exceed 5% in terms of the GPR peak, as shown in Table I. For the high-resistivity soil cases, which are more determinant for the estimation of the backflashover rate of the line, the deviations observed tend to reduce. This demonstrates the validity of the proposed counterpoise wire modeling approach using transmission line theory combined with Marti's model in ATP.

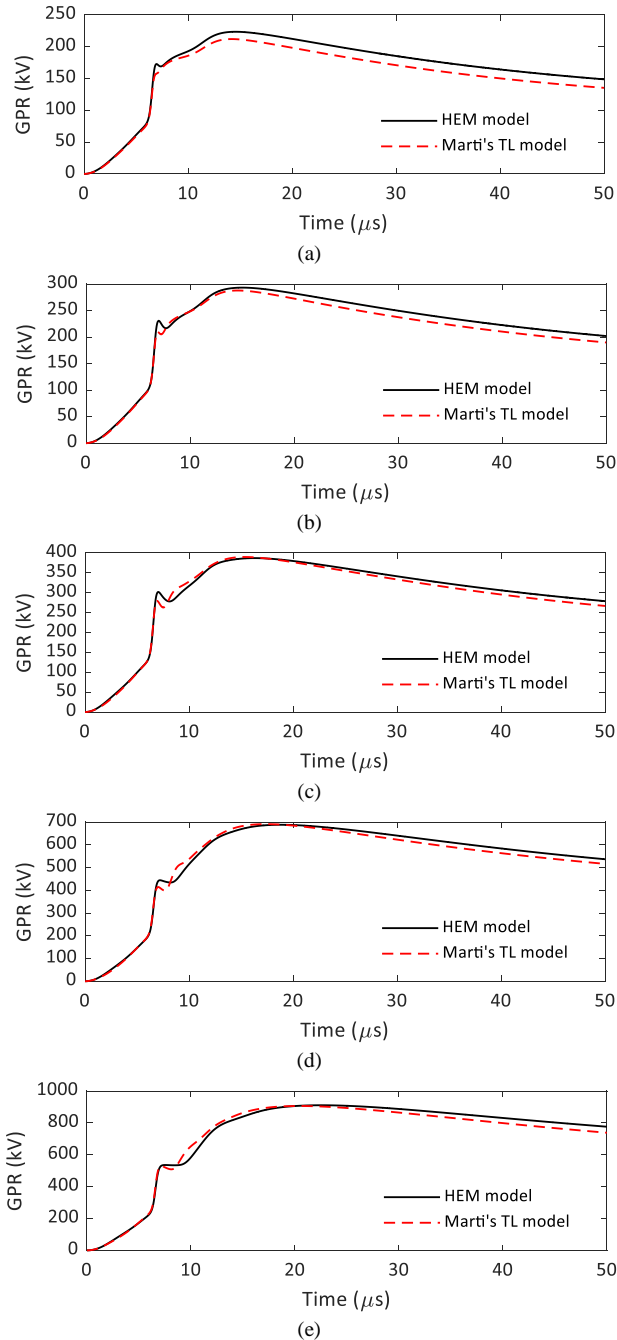


Fig. 6. GPRs developed by the tower-foot grounding system in response to the injection of the current shown in Fig 2 considering the proposed TL line model and the HEM model, and soil resistivities of (a) 250 Ωm , (b) 500 Ωm , (c) 1000 Ωm , (d) 2500 Ωm , and (e) 5000 Ωm .

TABLE I
PEAK VALUE OF THE GPR

ρ (Ωm)	250	500	1000	2500	5000
V_p (kV) Marti's TL model	212	288	390	691	906
V_p (kV) HEM model	223	293	387	688	911
$ \Delta $ (%)	4.9	1.7	0.8	0.4	0.5

D. Comparison with the Gatta et al.'s Model

To further assess the applicability and the accuracy of the proposed model, the results it provides are compared with those obtained using a previous model available in literature. In [11], a pi-equivalent circuit, as shown in Fig. 7(a), is proposed to simulate the transient response of typical grounding configurations of Italian transmission lines. The parameters of the pi-circuit are estimated by an optimization procedure, taking as reference a full circuit model. Considering the configuration shown in Fig. 7(b), and constant ground parameters with $\rho_g = 1000 \Omega$ and $\epsilon_{rg} = 35$, the following parameters were determined [11]: $R_1 = 34.122 \Omega$, $R_2 = 43.266 \Omega$, $C_1 = 3.32 \text{ nF}$, $C_2 = 9.00 \text{ nF}$, $R = 0$, and $L = 12.50 \mu\text{H}$. The voltage-controlled current sources G_1 and G_2 accounts for soil ionization and were not considered in this paper.

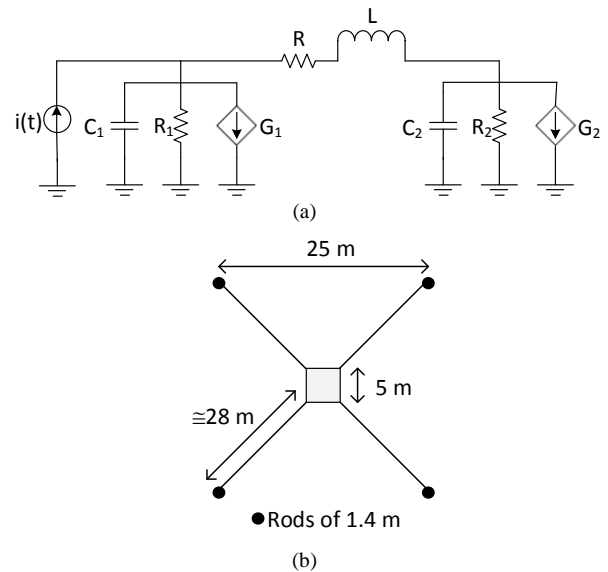


Fig. 7. (a) Pi-equivalent circuit model. (b) Grounding system composed of four horizontal conductors made of strap iron (40 mm \times 4 mm) buried at 0.8 m depth. In the proposed model, the length of the rods connected at the end were incorporated into the total length of the horizontal electrodes.

Fig. 8 compares the GPRs calculated with the proposed and the pi-circuit models in response to the current waveform depicted in Fig. 2. In the case of the proposed model, two curves are presented, one considering and the other disregarding the exponential term in (4). For comparison purposes, the result obtained with the HEM reference model is also included. In general, the obtained results are in good agreement. If the exponential term is considered a small difference of around 4% between the peaks of the GPRs computed using the proposed and the pi-circuit models is observed, although the former leads to better agreement with

the HEM model. Along the tail, the models are nearly coincident, which indicates that they basically lead to the same value of the low-frequency grounding resistance.

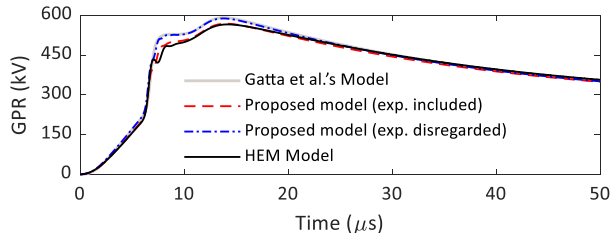


Fig. 8. Comparison between the simulated GPRs developed by the grounding system shown in Fig. 7(b) in response to the current shown in Fig. 2, considering the proposed model and the pi-circuit model proposed in [11].

Finally, it should be noted that, although the model proposed here has been applied to evaluate the typical grounding configuration of TL towers illustrated in Fig. 3, it can be applied to other grounding arrangements as long as they can be approximately represented by parallel conductors.

IV. ASSESSMENT OF THE LIGHTNING PERFORMANCE OF THE TRANSMISSION LINE

In order to further demonstrate the applicability and accuracy of the tower-foot grounding model, the lightning performance of the transmission line in terms of its outage rate is assessed in this Section. The transmission system is modeled in ATP and the resulting lightning overvoltages due to a direct strike to the tower are computed considering two grounding models, one based on the transmission line theory as proposed in this paper and the other based on the rigorous representation provided by HEM. Finally, the estimated outage rates are computed and compared.

A. Modeling of Transmission Line Components

As detailed in [8], the tower geometry depicted in Fig. 1 was divided into four sections connected in cascade, each one modeled as a single-phase distributed-parameter line. Each section is represented by four vertical parallel conductors, and the equivalent surge impedance of the associated single-phase line is computed applying the modified Jordan's formula [32]. The following surge impedances were obtained for each section from the bottom to the top of the tower: $Z_1 = 121 \Omega$, $Z_2 = 171 \Omega$, $Z_3 = 223 \Omega$, and $Z_4 = 272 \Omega$.

The simulations assume direct lightning strikes to the top of a central tower of the system and five spans at each side of the strike point are considered. Each span is represented as an untransposed line section with distributed/frequency-dependent parameters. Long lines are connected to the last towers of each side to avoid reflections that could affect the simulated overvoltages along the struck tower. Fig. 9 depicts a schematic representation of the simulated system.

The tower-foot grounding system is modeled in two different ways. One is the model described in Section III, which considers Sunde's equations applied to bare buried conductors along with Marti's line model (labeled henceforth as "Marti's TL model"). The other model, assumed as a benchmark, corresponds to the grounding system

representation by its frequency-dependent input impedance computed using the accurate electromagnetic model (labeled henceforth as "HEM model") [28]. In this work, this impedance is calculated in a frequency range from 1 Hz to 10 MHz and incorporated in the ATP time-domain simulations through an equivalent circuit as detailed in [7], [8], [33].

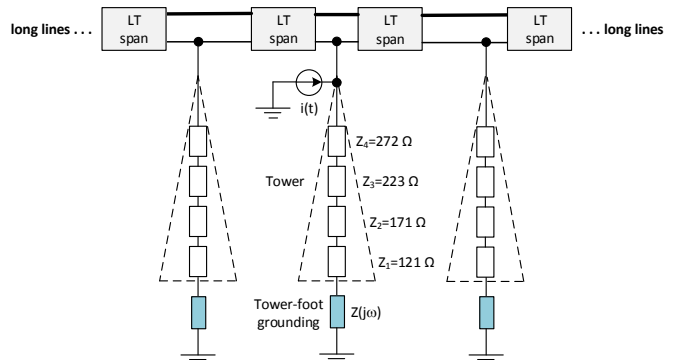


Fig. 9. Schematic representation of the simulated system corresponding to a direct strike to the top of a tower flanked by adjacent towers (only two represented in the figure).

B. Simulated Overvoltages

Fig. 10 shows the lightning overvoltages across the lower phase insulator of the line, which is the critical phase, in response to a direct strike at the tower top considering the median first stroke current of Fig. 2. The lightning overvoltages were determined considering the two tower-foot grounding models investigated in this paper.

The results indicate an excellent agreement between the simulated overvoltages considering the proposed grounding model based on transmission line theory and the HEM model. As shown in Table II, the differences between the peak values (V_P) of the simulated overvoltages using the two different approaches for the tower-foot grounding modeling are less than 3% and show a slight increase with increasing soil resistivity. This stems from the fact the overvoltages across line insulators are markedly influenced by the tower-foot impedance, notably by the reflection coefficient at the bottom of the tower given by $\Gamma = (Z_G - Z_T)/(Z_G + Z_T)$, where Z_G is the tower-foot grounding impedance and Z_T is the tower surge impedance. The relative sensitivity of the reflection coefficient, $\frac{\partial \Gamma / \partial Z_G}{\Gamma}$, increases with Z_G ; thus, it is more sensitive in case of high-resistivity soils, which are associated with higher values of tower-foot impedance. Thus, even small deviations observed between the two grounding models for high-resistivity soils, as shown in Section III-C, can lead to larger percentage differences between the simulated peak overvoltage values developed across the insulator strings. Anyway, the observed errors are quite small and are within the uncertainties present in the estimation of the lightning performance of transmission lines.

Finally, it is noteworthy that a good agreement between the simulated overvoltages is observed not only along the front of the waveforms, but also along their tails. This indicates that the proposed tower-foot grounding model may be also suitable for lightning studies involving energy stress, such as the energy dissipated by surge arresters [34].

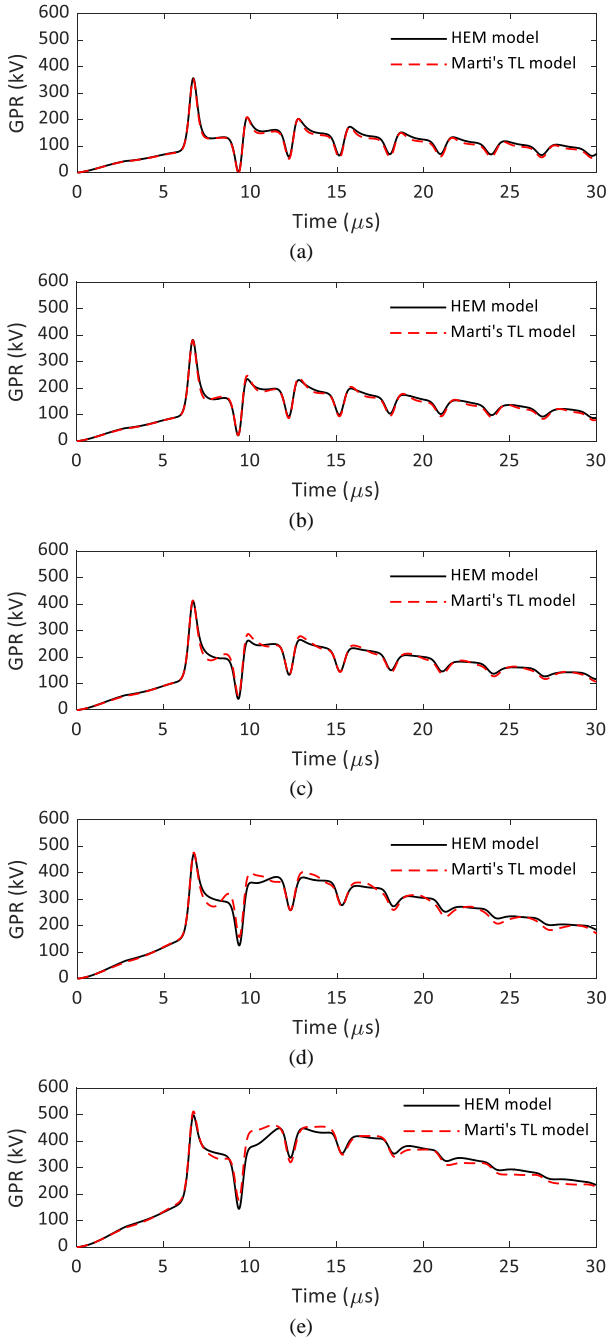


Fig. 10. Lightning overvoltages developed across the lower line insulator, considering the proposed TL line model and the HEM model, and soil resistivities of (a) 250 Ωm , (b) 500 Ωm , (c) 1000 Ωm , (d) 2500 Ωm , and (e) 5000 Ωm .

TABLE II
PEAK VALUE OF THE OVERVOLTAGES ACROSS THE LOWER INSULATOR

ρ (Ωm)	250	500	1000	2500	5000
V_p (kV) Marti's TL model	353	381	414	476	512
V_p (kV) HEM model	356	382	411	470	498
$ \Delta $ (%)	0.8	0.3	0.7	1.3	2.8

C. Backflashover Rate of the Line

The main parameter that measures the TL performance is its outage rate per 100 km per year. To compute this rate, results similar to those shown in Fig. 10 were obtained by

varying the peak current amplitude. For each peak current value, the integration method was applied to the impinging overvoltages across the line insulators to check whether insulation breakdown will occur or not [35]. The peak value of the lightning current that causes insulation breakdown leading to line outage is called critical current I_C . Then, the line backflashover rate assuming a given value of ground resistivity is computed as

$$BFR_k = 0.6 \times N_L \times P(I_p > I_{Ck}) \quad (11)$$

where BFR_k is the backflashover rate considering a ground resistivity ρ_k , $P(I_p > I_{Ck})$ is the probability of the lightning peak current being greater than the minimum current that causes insulation breakdown, the factor 0.6 is used to disregard the effect of strokes along the span, and N_L is the expected number of flashes to the line per 100 km per year. Finally, the global line backflashover rate is given by

$$BFR = \frac{1}{N} \sum_{k=1}^{N_p} BFR_k \times N_k \quad (12)$$

where N_p is the number of sections into which the line is divided with representative resistivity ρ_k , N_k is the percentage of towers located in a section with resistivity ρ_k , and $N = N_1 + N_2 + \dots + N_k = 100$. More details on the calculation of line outage rate can be found in standards [1], [5].

Table III presents the results of the expected backflashover rate, assuming four different possibilities of ground resistivity distributions along the line route and considering the two approaches for tower-foot grounding modeling. The results were obtained considering the Berger's cumulative peak current distribution [14], [15] and a normalized ground flash density of 1 flash/ km^2/year . The parameter Δ in the table indicates the absolute percentage differences between the results obtained considering the two tower-foot grounding models.

TABLE III
ESTIMATED BACKFLASHOVER RATES

Number	Percentual distribution of soils with different resistivity along the transmission line route (%)					BFR		$ \Delta $ (%)
	250	500	1000	2500	5000	TL Marti's model	HEM model	
1	30	40	30	0	0	0.62	0.63	1.6
2	0	0	40	30	30	2.03	1.97	3.0
3	20	20	20	20	20	1.47	1.45	1.4
4	10	25	30	25	10	1.36	1.33	2.3

According to the results, a good agreement between the estimated backflashover rates, considering the two approaches for the tower-foot grounding modeling, is observed. Notably, this good agreement is observed for all considered ground resistivity distributions which describe different scenarios. For instance, distribution 1 comprises soils of low and moderate resistivity, while in distribution 2 soils of high resistivity predominate. Distribution 3 describes a uniform ground resistivity scenario and distribution 4 presents a symmetry of ground resistivity values around 1000 Ωm .

V. CONCLUSIONS

This paper proposes a model for tower-foot grounding systems based on the application of transmission line theory and Marti's model. The good accuracy of the proposed model is demonstrated using an electromagnetic model as a benchmark. The model is implemented in ATP, allowing the simulation of lightning overvoltages using models already available on this platform. It is shown that good results are obtained both along the front and tail of the overvoltage waveforms. This suggests that the proposed model can be conveniently used in general lightning transient studies without incurring in significant errors. Although a typical tower-foot grounding configuration composed of horizontal counterpoise wires was taken as reference, similar conclusions could be drawn for an arrangement composed of vertical rods, for instance. More importantly, the proposed model is EMT-program compatible, and might support the implementation of an electrical grounding component in time-domain simulators. Finally, since voltages and currents are readily available at both ends of the counterpoise wires, short grounding sections could be cascaded for determining current distributions required for calculating electromagnetic fields in the vicinity of the grounding electrodes, or for allowing multiple current injection points.

VI. REFERENCES

- [1] IEEE Std 1243-1997, "IEEE Guide for Improving the Lightning Performance of Transmission Lines," New York, 1997.
- [2] Z. G. Datsios, P. N. Mikropoulos, and T. E. Tsovilis, "Closed-form expressions for the estimation of the minimum backflashover current of overhead transmission lines," *IEEE Trans. Power Deliv.*, vol. 36, no. 2, pp. 522–532, 2021.
- [3] S. Visacro and F. H. Silveira, "Lightning Performance of Transmission Lines: Requirements of Tower-Footing Electrodes Consisting of Long Counterpoise Wires," *IEEE Trans. Power Deliv.*, vol. 31, no. 4, pp. 1524–1532, Aug. 2016.
- [4] A. Ametani and T. Kawamura, "A Method of a Lightning Surge Analysis Recommended in Japan Using EMTP," *IEEE Trans. Power Deliv.*, vol. 20, no. 2, pp. 867–875, Apr. 2005.
- [5] Working Group C4.23, "CIGRE TB 839: Procedures for Estimating the Lightning Performance of Transmission Lines – New Aspects," Paris, 2021.
- [6] L. Grcev, "Impulse Efficiency of Ground Electrodes," *IEEE Trans. Power Deliv.*, vol. 24, no. 1, pp. 441–451, Jan. 2009.
- [7] M. R. Alemi and K. Sheshyekani, "Wide-Band Modeling of Tower-Footing Grounding Systems for the Evaluation of Lightning Performance of Transmission Lines," *IEEE Trans. Electromagn. Compat.*, vol. 57, no. 6, pp. 1627–1636, Dec. 2015.
- [8] R. Alipio, A. De Conti, N. Duarte, and F. Rachidi, "Influence of a lossy ground on the lightning performance of overhead transmission lines," *Electr. Power Syst. Res.*, vol. 214, p. 108951, Jan. 2023.
- [9] Y. Liu, N. Theethayi, and R. Thottappillil, "An Engineering Model for Transient Analysis of Grounding System Under Lightning Strikes: Nonuniform Transmission-Line Approach," *IEEE Trans. Power Deliv.*, vol. 20, no. 2, pp. 722–730, Apr. 2005.
- [10] L. Grcev and M. Popov, "On High-Frequency Circuit Equivalents of a Vertical Ground Rod," *IEEE Trans. Power Deliv.*, vol. 20, no. 2, pp. 1598–1603, Apr. 2005.
- [11] F. M. Gatta, A. Geri, S. Lauria, and M. Maccioni, "Simplified HV tower grounding system model for backflashover simulation," *Electr. Power Syst. Res.*, vol. 85, pp. 16–23, Apr. 2012.
- [12] J. Marti, "Accurate Modelling of Frequency-Dependent Transmission Lines in Electromagnetic Transient Simulations," *IEEE Trans. Power Appar. Syst.*, vol. PAS-101, no. 1, pp. 147–157, Jan. 1982.
- [13] A. De Conti and S. Visacro, "Analytical Representation of Single- and Double-Peaked Lightning Current Waveforms," *IEEE Trans. Electromagn. Compat.*, vol. 49, no. 2, pp. 448–451, May 2007.
- [14] K. Berger, R. B. Anderson, and H. Kroninger, "Parameters of lightning flashes," *Electra*, no. 80, pp. 223–237, 1975.
- [15] Working Group C4.407, "CIGRE TB 549: Lightning parameters for engineering applications," CIGRE, Paris, 2013.
- [16] E. D. Sunde, *Earth Conduction Effects in Transmission Systems*. New York: Dover Publications, 1968.
- [17] L. Grcev and S. Grceva, "On HF Circuit Models of Horizontal Grounding Electrodes," *IEEE Trans. Electromagn. Compat.*, vol. 51, no. 3, pp. 873–875, Aug. 2009.
- [18] J. Osvaldo Saldanha Paulino, W. do C. Boaventura, A. Barros Lima, and Maurissone Ferreira Guimaraes, "Transient voltage response of ground electrodes in the time-domain," in *2012 International Conference on Lightning Protection (ICLP)*, Sep. 2012, pp. 1–6.
- [19] C. E. F. Caetano, A. B. Lima, J. O. S. Paulino, W. C. Boaventura, and E. N. Cardoso, "A conductor arrangement that overcomes the effective length issue in transmission line grounding," *Electr. Power Syst. Res.*, vol. 159, pp. 31–39, Jun. 2018.
- [20] S. A. Schelkunoff, "The Electromagnetic Theory of Coaxial Transmission Lines and Cylindrical Shields," *Bell Syst. Tech. J.*, vol. 13, no. 4, pp. 532–579, Oct. 1934.
- [21] R. King, "Antennas in material media near boundaries with application to communication and geophysical exploration, Part I: The bare metal dipole," *IEEE Trans. Antennas Propag.*, vol. 34, no. 4, pp. 483–489, Apr. 1986.
- [22] F. Rachidi and S. Tkachenko, "Electromagnetic Field Interaction with Transmission Lines – From Classical Theory to HF Radiation Effects", WIT Press, 2008.
- [23] L. M. Wedepohl, "Application of matrix methods to the solution of travelling-wave phenomena in polyphase systems," *Proc. Inst. Electr. Eng.*, vol. 110, no. 12, p. 2200, 1963.
- [24] B. Gustavsen and A. Semlyen, "Rational approximation of frequency domain responses by vector fitting," *IEEE Trans. Power Deliv.*, vol. 14, no. 3, pp. 1052–1061, Jul. 1999.
- [25] A. De Conti and M. P. S. Emidio, "Extension of a modal-domain transmission line model to include frequency-dependent ground parameters," *Electr. Power Syst. Res.*, vol. 138, pp. 120–130, Sep. 2016.
- [26] R. Alipio and S. Visacro, "Modeling the Frequency Dependence of Electrical Parameters of Soil," *IEEE Trans. Electromagn. Compat.*, vol. 56, no. 5, pp. 1163–1171, Oct. 2014.
- [27] B. Gustavsen, "Passivity Enforcement for Transmission Line Models Based on the Method of Characteristics," *IEEE Trans. Power Deliv.*, vol. 23, no. 4, pp. 2286–2293, Oct. 2008.
- [28] S. Visacro and A. Soares, "HEM: A Model for Simulation of Lightning-Related Engineering Problems," *IEEE Trans. Power Deliv.*, vol. 20, no. 2, pp. 1206–1208, Apr. 2005.
- [29] Working Group C4.37, "CIGRE TB 785: Electromagnetic computation methods for lightning surge studies with emphasis on the FDTD method," Paris, 2019.
- [30] S. Visacro, R. Alipio, C. Pereira, M. Guimaraes, and M. A. O. Schroeder, "Lightning Response of Grounding Grids: Simulated and Experimental Results," *IEEE Trans. Electromagn. Compat.*, vol. 57, no. 1, pp. 121–127, Feb. 2015.
- [31] R. Alipio, D. Conceição, A. De Conti, K. Yamamoto, R. N. Dias, and S. Visacro, "A comprehensive analysis of the effect of frequency-dependent soil electrical parameters on the lightning response of wind-turbine grounding systems," *Electr. Power Syst. Res.*, vol. 175, p. 105927, Oct. 2019.
- [32] A. De Conti, S. Visacro, A. Soares, and M. A. O. Schroeder, "Revision, Extension, and Validation of Jordan's Formula to Calculate the Surge Impedance of Vertical Conductors," *IEEE Trans. Electromagn. Compat.*, vol. 48, no. 3, pp. 530–536, Aug. 2006.
- [33] B. Gustavsen, "Computer code for rational approximation of frequency dependent admittance matrices," *IEEE Trans. Power Deliv.*, vol. 17, no. 4, pp. 1093–1098, Oct. 2002.
- [34] J. A. Martinez and F. Castro-Aranda, "Lightning Flashover Rate of an Overhead Transmission Line Protected by Surge Arresters," in *2007 IEEE Power Engineering Society General Meeting*, Jun. 2007, pp. 1–6.
- [35] A. R. Hileman, *Insulation Coordination for Power Systems*, 1 edition. CRC Press, 1999.